ORIGINAL ARTICLE

A C G publications

Org. Commun. 17:1 (2024) 23-37

organic communications

Synthesis, characterization and biological activity of novel ionic liquids with bis-imidazole moieties: antitumor, antimicrobial effects and molecular docking studies

Fatih Çelik [1], Yasemin Ünver [1,*] Ali Aydın[b] [2] Halil İbrahim Güler and Kadriye İnan Bektaş [3]

[1]*Department of Chemistry, Faculty of Sciences, Karadeniz Technical University, 61080 Trabzon, Türkiye*

[2]*Department of Basic Medical Science, Faculty of Medicine, Bozok University, 66100, Yozgat, Türkiye*

[3]*Department of Molecular Biology and Genetics, Karadeniz Technical University Faculty of Science, 61080-Trabzon, Türkiye*

(Received January 04, 2024; Revised March 20, 2024; Accepted March 21, 2024)

Abstract: In this study, bis-Schiff bases with imidazole (**2**) and bis-imidazolium liquids (**3a-g**) were synthesized. The new compounds were characterized by Fourier transform infrared (FTIR), proton and carbon-13 nuclear magnetic resonance spectroscopy (^{1}H- and ^{13}C- NMR). The MTT assay was performed by our research group to measure the anticancer effect of the synthesized molecules on cell proliferation (NCI-60 screening method). Accordingly, when molecules **3e**, **3g** and **3f** were compared with other molecules and 5-Fluorouracil (5FU) (positive control), they were found to exhibit potent anticancer activity against all cancer cell lines ((Growth inhibition (GI50): 1.0 - 1.82, total growth inhibition (TGI): 1.09 - 4.79 and lethal concentration (LC50): 2.74 – 59.5 µg/mL), but also a strong cytotoxic effect on normal lung cells Beas2B and normal cartilage cells HC (GI50: 1.0 - 1.28, TGI: 1.03 - 2.61 and LC50: 1.77 - 41.7 µg/mL). The in vitro antimicrobial activity of the synthesized compounds was evaluated against a range of microorganisms, including four Gram-positive bacteria (*B. cereus*, *S. aureus*, *E. faecalis*, *B. subtilis*), four Gram-negative bacteria (Y. pseudotuberculosis, P. aeruginosa, E. coli, K. pneumoniae) and two yeast-like fungi (*C. albicans, C. tropicalis*). Molecular docking calculations were performed to investigate the ligand-protein interactions between the compounds and the Epidermal Growth Factor Receptor (EGFR) and the Vascular Endothelial Growth Factor Receptor (VEGFR1).

Keywords: Bis imidazolium ionic liquids; anticancer effects; antimicrobial activity; molecular docking.

1. Introduction

It is known that compounds containing imidazole have a fairly widespread biological capacity. Histidine is an imidazole derivative, (β-4-imidazolanine) is an important α-amino acid. Histamine, a

* Corresponding author: E-mail: unver.yasemincan@hotmail.com (Y. Ünver); Phone: +90 4623772485

The article was published by ACG Publications
http://www.acgpubs.org/journal/organic-communications © January-March 2024 EISSN:1307-6175
DOI: http://doi.org/10.25135/acg.oc.163.2401.4014
Available online: March 26, 2024

derivative of histidine, is a hormonal compound that triggers allergies in the human body. Adenine and guanine are important imidazole derivatives in the nucleic acids found in the cell structure. The synthesis and design of new substances is of great importance due to the resistance that fungi quickly develop against antifungal substances. In this context, many azole derivatives have been synthesized in recent years. Bifanazole, for example, is an imidazole derivative that has been synthesized in recent years. It has been identified as the antifungal with the broadest spectrum of activity in clinical use and has a high selectivity.

Another important antifungal agent currently used in the treatment of systemic mucormycosis is fluconazole, ketoconazole, sertacanazole and miconazole belong to the class of important antifungal agents with ether bridges.[1-4] Ionic liquids, which are composed of anions and cations, have a very low melting point or can be liquid at room temperature, tend to decompose only at high temperatures.[5] In addition, they are accepted as important compounds due to their superior physical properties, as they are environmentally friendly organic solvents, have high viscosity and density, are non-volatile and non-flammable, and have high conductivity.

Recently, the significance of ionic liquids has grown due to their diverse applications: serving as organic biocatalysts, being utilized as battery fillers in electrochemistry, finding extensive use in analytical chemistry as metal binders, their ready availability, and their capability to mix with both organic solvents and water. This has made them crucial for synthesizing alternative compounds exhibiting ionic liquid characteristics.[6-9] The most common types of ionic liquids are imidazolium ionic liquids. Imidazolium-containing ionic liquids have many applications in synthesis chemistry, catalysis, extraction/separation processes, biocatalyst in biochemistry and battery filling in electrochemistry. These ionic liquids are generally obtained from the reaction of alkyl halides with N-Alkyl imidazole compounds. A general reaction in which monocationic ionic liquids containing imidazolium cation and halide anion are synthesized from the reaction of an equivalent amount of alkyl halide and N-Alkyl imidazole compound is shown below.[10-12]

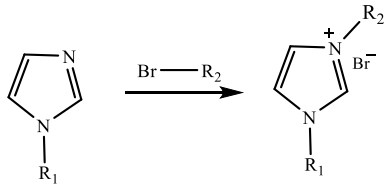

Scheme 1. Ionic liquids containing imidazolium cation and halide anion

This manuscript focuses on synthesizing imidazolium ionic liquids and explores how their biological activities are influenced by the length of the hydrocarbon chain and their solubility. The synthesis process is outlined, and the compounds' structures are determined using IR and NMR spectroscopy. Additionally, the manuscript aims to include studies on the antitumor and antimicrobial activities of these compounds to further enrich its content. Molecular docking calculations were performed to study the ligand-protein interactions.

2. Experimental

*2.1. Synthesis of (1E,1'E)-1,1'-(1,4-phenylene)bis(N-(3-(1H-imidazol-1-yl)propyl)methanimine) (**2**)*:

3-(1H-imidazol-1-yl)propan-1-amine (2 mol) and terephthalaldehyde (1 mol) were added to the flask and mixed by controlled heating in an oil bath at 160-170 ^{0}C. After 2 hours, the reaction was stopped and cooled. The reaction time was determined by thin layer chromatography (TLC) (ethyl alcohol-ethyl acetate). The precipitate was purified from DMSO-H_2O (1:2). (Scheme 1). Yield, 90.80 %, m.p. 93-95 ^{0}C. IR (KBr, cm^{-1}): 3100 (=CH), 2973,2956,2921 (-CH), 1645 (C=N), 1504 (C=C); ^{1}H NMR (400 MHz, DMSO-d_6) δ: 2.05-2.12 (m, 2CH_2-C<u>H</u>$_2$-CH_2-imid., 4H), 3.54 (t, 2C<u>H</u>$_2$-CH_2-CH_2-imid., 4H), 4.07 (t, 2CH_2-CH_2-C<u>H</u>$_2$-imid., 4H), benzene H [7.83 (s, 4H)], imid. H [(6.89 (s, 2H), 7.22 (s, 2H), 7.65 (s, 2H)], 8.38 (s, 2N=CH, 2H); ^{13}C NMR (100 Hz, DMSO-d_6) δ: 32.22(CH_2-<u>C</u>H_2-CH_2-imid.), 44.50 (CH_2-CH_2-

CH_2-imid.), 57.48 (CH_2-CH_2-CH_2-imid.), benzene C [128.64 (4CH), 138.66 (2C)], imid. C [(119.47 (2CH), 128.89 (2CH), 137.23 (2CH)], 160.81 (2N=CH).

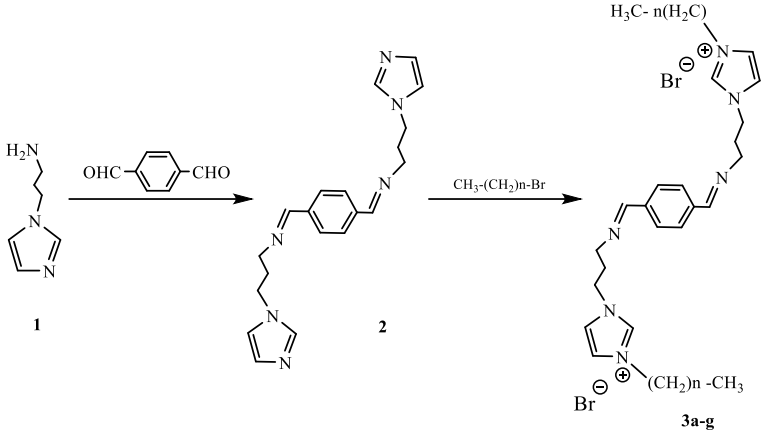

n	3	4	5	6	7	8	9
	a	b	c	d	e	f	g

Scheme 2. Synthetic pathway of imidazolium ionic liquids **2**,3(**a**-**g**)

*2.2 Synthesis of bis (3-alkyl-1H-imidazol-3-ium) bis bromide (**3a-g**)*

1E,1'E)-1,1'-(1,4-phenylene) bis (N-(3-(1H-imidazol-1-yl)propyl) methanimine) and alkyl bromide (butyl-decyl bromide) were mixed in an oil bath in a carboy by heating in the temperature range of 160-170 ^{0}C. The reaction, which was controlled by TLC, was stopped and cooled after 2 hours. The oily content of the balloon was washed several times with hot acetone, cleaned and dried in a desiccator.

*2.2.1 1,1'-((((1E,1'E)-1,4-phenylenebis(methanylylidene))bis(azanylydiene)bis(propane-3,1-diyl)bis(3-butyl-1H-imidazol-3-ium) bis bromide (**3a**)*: Yield: 78.50%. IR (KBr, cm^{-1}): 3074 (=CH), 2958, 2872 (-CH), 1640 (C=N), 1562 (C=C); ^{1}H NMR (400 MHz, DMSO-d_6) δ: butyl H [(0.88 (bs, 2CH_3, 6H), 1.24 (bs, 2CH_2, 4H), 1.77 (bs, 2CH_2, 4H), 4.33 (bs, 2CH_2, 4H)], 2.20 (bs, 2CH_2-CH_2-CH_2-imid., 4H), 3.54 (bs, 2CH_2-CH_2-CH_2-imid., 4H), 4.19 (bs, 2CH_2-CH_2-CH_2-imid., 4H), benzene H [7.89 (bs, 4H)], imid. H [(7.89 (bs, 4H), 8.43 (s, 2H)], 9.41 (s, 2N=CH, 2H); ^{13}C NMR (100 Hz, DMSO-d_6) δ: butyl C [13.76 (CH_3), 19.26 (CH_2), 29.04 (CH_2), 49.11 (CH_2)], 31.74 (CH_2-CH_2-CH_2-imid.), 47.94 (CH_2-CH_2-CH_2-imid.), 57.56 (CH_2-CH_2-CH_2-imid.), benzene C [128.62 (CH), 138.25 (C)], imid. C [122.76 (CH), 122.96 (CH), 128.62 (CH)], 161.75 (N=CH).

*2.2.2 1,1'-((((1E,1'E)-1,4-phenylenebis(methanylylidene))bis(azanylydiene)bis(propane-3,1-diyl)bis(3-pentyl-1H-imidazol-3-ium) bis bromide (**3b**)*: Yield: 67.80%. IR (KBr, cm^{-1}): 3075 (=CH), 2955, 2930 (-CH), 1639 (C=N), 1562 (C=C); ^{1}H NMR (400 MHz, DMSO-d_6) δ: pentyl H [(0.83 (bs, 2CH_3, 6H), 1.20-1.29 (m, 4CH_2, 8H), 1.76 (bs, 2CH_2, 4H), 4.34 (bs, 2CH_2, 4H)], 2.21 (bs, 2CH_2-CH_2-CH_2-imid., 4H), 3.63 (bs, 2CH_2-CH_2-CH_2-imid., 4H), 4.11 (bs, 2CH_2-CH_2-CH_2-imid., 4H), benzene H [7.79-7.90 (m, 4H)], imid. H [(7.79-7.90 (m, 4H), 8.42 (s, 2H)], 9.40 (s, 2N=CH, 2H); ^{13}C NMR (100 Hz, DMSO-d_6) δ: pentyl C [14.14 (CH_3), 21.95 (CH_2), 28.10 (CH_2), 29.43 (CH_2), 49.10 (CH_2)], 30.92 (CH_2-CH_2-CH_2-imid.), 47.93 (CH_2-CH_2-CH_2-imid.), 57.65 (CH_2-CH_2-CH_2-imid.), benzene C [128.34 (CH), 138.42 (C)], imid. C [122.82 (CH), 123.04 (CH), 128.34 (CH)], 161.93 (N=CH).

*2.2.3 1,1'-((((1E,1'E)-1,4-phenylenebis(methanylylidene))bis(azanylydiene)bis(propane-3,1-diyl)bis(3-hexyl-1H-imidazol-3-ium) bis bromide (**3c**)*: Yield: 70.65%. IR (KBr, cm^{-1}): 3077 (=CH), 2955, 2928 (-CH), 1640 (C=N), 1562 (C=C); ^{1}H NMR (400 MHz, DMSO-d_6) δ: hexyl H [(0.84 (bs, 2CH_3, 6H), 1.24 (bs, 6CH_2, 12H), 1.79 (bs, 2CH_2, 4H), 4.33 (bs, 2CH_2, 4H)], 2.21 (bs, 2CH_2-CH_2-CH_2-imid., 4H), 3.50 (bs, 2CH_2-CH_2-CH_2-imid., 4H), 4.19 (bs, 2CH_2-CH_2-CH_2-imid., 4H), benzene H [7.79-7.90 (m, 4H)], imid. H [(7.79-7.90 (m, 4H), 8.41 (s, 2H)], 9.36 (s, 2N=CH, 2H); ^{13}C NMR (100 Hz, DMSO-d_6) δ: hexyl C [14.28 (CH_3), 22.33 (CH_2), 25.61(CH_2), 29.71 (CH_2), 31.00 (CH_2), 49.27 (CH_2)], 31.00 (CH_2-CH_2-

CH_2-imid.), 47.86 (CH_2-CH_2-$\underline{C}H_2$-imid.), 57.56 ($\underline{C}H_2$-CH_2-CH_2-imid.), benzene C [128.61 (CH), 138.14 (C)], imid. C [122.89 (CH), 123.04 (CH), 128.61 (CH)], 161.61 (N=CH).

*2.2.4 1,1'-((((1E,1'E)-1,4-phenylenebis(methanylylidene))bis(azanylydiene)bis(propane-3,1-diyl)bis(3-heptyl-1H-imidazol-3-ium) bis bromide (**3d**)*: Yield: 79.35%. IR (KBr, cm^{-1}): 3083 (=CH), 2927, 2855 (-CH), 1640 (C=N), 1564 (C=C); 70.65%. ^{1}H NMR (400 MHz, DMSO-d_6) δ: heptyl H [(0.83 (bs, $2CH_3$, 6H), 1.22 (bs, $8CH_2$, 16H), 1.74 (bs, $2CH_2$, 4H), 4.36 (bs, $2CH_2$, 4H)], 2.20 (bs, $2CH_2$-$C\underline{H}_2$-CH_2-imid., 4H), 3.64 (bs, $2C\underline{H}_2$-CH_2-CH_2-imid., 4H), 4.14 (bs, $2CH_2$-CH_2-$C\underline{H}_2$-imid., 4H), benzene H [7.78-7.91 (m, 4H)], imid. H [(7.78-7.91 (m, 4H), 8.41 (s, 2H)], 9.41 (s, 2N=CH, 2H); ^{13}C NMR (100 Hz, DMSO-d_6) δ: heptyl C [14.36 (CH_3), 22.42 (CH_2), 25.87 (CH_2), 28.47 (CH_2), 29.75 (CH_2), 30.91 (CH_2), 49.26 (CH_2)], 31.48 (CH_2-$\underline{C}H_2$-CH_2-imid.), 47.92 (CH_2-CH_2-$\underline{C}H_2$-imid.), 57.66 ($\underline{C}H_2$-CH_2-CH_2-imid.), benzene C [128.60 (CH), 138.14 (C)], imid. C [122.89 (CH), 123.03 (CH), 128.60 (CH)], 161.60 (N=CH).

*2.2.5 1,1'-((((1E,1'E)-1,4-phenylenebis(methanylylidene))bis(azanylydiene)bis(propane-3,1-diyl)bis(3-octyl-1H-imidazol-3-ium) bis bromide (**3e**)*: Yied:78.89%. IR (KBr, cm^{-1}): 3079 (=CH), 2925, 2855 (-CH), 1640 (C=N), 1562 (C=C); ^{1}H NMR (400 MHz, DMSO-d_6) δ: octyl H [(0.84 (bs, $2CH_3$, 6H), 1.22 (bs, $10CH_2$, 20H), 1.79 (bs, $2CH_2$, 4H), 4.34 (bs, $2CH_2$, 4H)], 2.22 (bs, $2CH_2$-$C\underline{H}_2$-CH_2-imid., 4H), 3.63 (bs, $2C\underline{H}_2$-CH_2-CH_2-imid., 4H), 4.16 (bs, $2CH_2$-CH_2-$C\underline{H}_2$-imid., 4H), benzene H [7.79-7.89 (m, 4H)], imid. H [(7.79-7.90 (m, 4H), 8.41 (s, 2H)], 9.38 (s, 2N=CH, 2H); ^{13}C NMR (100 Hz, DMSO-d_6) δ: : octyl C [14.40 (CH_3), 22.51 (CH_2), 25.95 (CH_2), 28.78 (CH_2), 28.94 (CH_2), 29.77 (CH_2), 30.92 (CH_2), 49.27 (CH_2)], 31.63 (CH_2-$\underline{C}H_2$-CH_2-imid.), 47.92 (CH_2-CH_2-$\underline{C}H_2$-imid.), 57.66 ($\underline{C}H_2$-CH_2-CH_2-imid.), benzene C [128.60 (CH), 138.15 (C)], imid. C [122.90 (CH), 123.03 (CH), 128.60 (CH)], 161.62 (N=CH).

*2.2.6 1,1'-((((1E,1'E)-1,4-phenylenebis(methanylylidene))bis(azanylydiene)bis(propane-3,1-diyl)bis(3-nonyl-1H-imidazol-3-ium) bis bromide (**3f**)*: Yield:77.68%. IR (KBr, cm^{-1}): 3042 (=CH), 2923, 2851 (-CH), 1643 (C=N), 1563 (C=C); ^{1}H NMR (400 MHz, DMSO-d_6) δ: nonyl H [(0.84 (bs, $2CH_3$, 6H), 1.22 (bs, $12CH_2$, 24H), 1.77 (bs, $2CH_2$, 4H), 4.34 (bs, $2CH_2$, 4H)], 2.21 (bs, $2CH_2$-$C\underline{H}_2$-CH_2-imid., 4H), 3.63 (bs, $2C\underline{H}_2$-CH_2-CH_2-imid., 4H), 4.11 (bs, $2CH_2$-CH_2-$C\underline{H}_2$-imid., 4H), benzene H [7.79-7.90 (m, 4H)], imid. H [(7.79-7.90 (m, 4H), 8.41 (s, 2H)], 9.38 (s, 2N=CH, 2H); ^{13}C NMR (100 Hz, DMSO-d_6) δ: nonyl C [14.41 (CH_3), 22.54 (CH_2), 25.95 (CH_2), 28.82 (CH_2), 29.04 (CH_2), 29.25 (CH_2), 29.74 (CH_2), 31.70 (CH_2), 49.27 (CH_2)], 30.93 (CH_2-$\underline{C}H_2$-CH_2-imid.), 47.92 (CH_2-CH_2-$\underline{C}H_2$-imid.), 57.66 ($\underline{C}H_2$-CH_2-CH_2-imid.), benzene C [128.60 (CH), 138.16 (C)], imid. C [122.91 (CH), 123.05 (CH)], 161.62 (N=CH).

*2.2.7 1,1'-((((1E,1'E)-1,4-phenylenebis(methanylylidene))bis(azanylydiene)bis(propane-3,1-diyl)bis(3-decyl-1H-imidazol-3-ium) bis bromide (**3g**)*: Yield:75.65%. IR (KBr, cm^{-1}): 3041 (=CH), 2955, 2922 (-CH), 1643 (C=N), 1562 (C=C); ^{1}H NMR (400 MHz, DMSO-d_6) δ: decyl H [(0.84 (bs, $2CH_3$, 6H), 1.22 (bs, $14CH_2$, 28H), 1.76 (bs, $2CH_2$, 4H), 4.38 (bs, $2CH_2$, 4H)], 2.19 (bs, $2CH_2$-$C\underline{H}_2$-CH_2-imid., 4H), 3.61 (bs, $2C\underline{H}_2$-CH_2-CH_2-imid., 4H), 4.11 (bs, $2CH_2$-CH_2-$C\underline{H}_2$-imid., 4H), benzene H [7.80-7.88 (m, 4H)], imid. H [(7.80-7.88 (m, 4H), 8.41 (s, 2H)], 9.33 (s, 2N=CH, 2H); ^{13}C NMR (100 Hz, DMSO-d_6) δ: decyl C [14.42 (CH_3), 22.55 (CH_2), 25.82 (CH_2), 28.81 (CH_2), 29.13 (CH2), 29.29 (CH2), 29.34 (CH_2), 29.72 (CH_2), 31.74 (CH_2), 49.29 (CH_2)], 30.93 (CH_2-$\underline{C}H_2$-CH_2-imid.), 47.87 (CH_2-CH_2-$\underline{C}H_2$-imid.), 57.65 ($\underline{C}H_2$-CH_2-CH_2-imid.), benzene C [128.61 (CH), 138.26 (C)], imid. C [122.83 (CH), 123.06 (CH)], 161.72 (N=CH).

3. Results and Discussion

3.1. Synthesis

In the first step of synthesis, Schiff base (**2**) was produced by condensing terephthalaldehyde with aminoimidazole in an oil bath. Analysis of the IR and H NMR spectra did not reveal bands

corresponding to aldehyde and amino groups. Instead, the NMR spectra exhibited a proton signal for the CH=N group of the imine at 8.38 ppm and a carbon signal at 160.81 ppm.

In the subsequent synthesis step, compounds 3 were obtained by reacting compound **2** with alkyl halides. The 1H NMR spectra of compounds 3 displayed proton signals from the alkyl groups within the expected range of 0.83-4.36 ppm. Corresponding carbon signals were observed in the range of 14.28-49.29 ppm. The structures of compounds 3 were further confirmed by their ^{1}H and ^{13}C NMR data.

3.2.Antitumor Activity

3.2.1. Evaluation of New Molecules According to NCI60 Screening Methodology

The MTT test was performed to measure the anticancer effects of synthesized molecules by our research group on cell proliferation (NCI-60 screening methodology). Accordingly, when comparing **3e** (GI50: 1.00 - 1.48, TGI: 1.09 - 3.99, and LC50: 2.91 - 140.6 µg/mL), **3g** (GI50: 1.00 - 1.22, TGI: 1.12 - 3.15, and LC50: 2.74 - 137.1 µg/mL), and **3f** (GI50: 1.01 - 1.82, TGI: 1.15 - 4.79, and LC50: 3.55 - 109.3 µg/mL) molecules to other molecules and 5FU (positive control), it was figured out they showed a powerful anticancer effect against all cancer cell lines, but also they caused a highly cytotoxic effect on normal lung Beas2B cells (GI50: 1.00 - 1.26, TGI: 1.03 - 1.92, and LC50: 1.77 - 6.37 µg/mL) and normal chondrocyte HC cells (GI50: 1.10 - 1.28, TGI: 1.70 - 2.61, and LC50: 17.02 - 41.7 µg/mL) (Table 1, 2, and 3).

Table 1. GI50, TGI, and LC50 values (as µg/mL) for tested compounds against A549, Calu1, and H1650*

Compound	A549**			Calu1**			H1650**		
	GI50	**TGI**	**LC50**	**GI50**	**TGI**	**LC50**	**GI50**	**TGI**	**LC50**
3e	1.02	1.38	64.7±2.4	1.48	3.99	129.3±4.9	1.16	3.14	140.6±6.1
2	1.67	18.7±1.0	>500	1.09	2.49	>500	1.17	3.53	>500
3g	1.15	2.02	31.7±1.6	1.00	1.12	32.3±1.5	1.22	3.15	137.1±4.8
3b	1.22	44.8±1.8	>500	1.00	81.3±3.7	>500	3.04	324.8±11.3	>500
3c	1.05	49.2±1.7	>500	2.98	198.2±8.5	>500	1.50	31.2±1.5	>500
3d	1.37	26.6±1.1	>500	1.11	2.32	>500	1.48	7.82	>500
3f	1.42	3.62	109.3±4.8	1.05	1.81	102.3±4.0	1.31	2.81	49.9±2.0
3a	1.25	33.1±1.9	>500	1.06	12.5±0.6	>500	1.20	84.6±3.0	>500
5FU	1.44	47.1±1.7	470.0±18	1.72	61.8±3.1	450.4±16	1.55	28.6±1.4	392.0±14.2

*Percent inhibition noted is mean values ± SDs of three independent measures.
** If percent inhibition is smaller than 10, the SD value is <0.5.

Actually, if these **3e**, **3g**, and **3f** molecule's toxic effects against normal cells are reduced by chemical by modifying, they may be a good option for cancer treatment. Interestingly, when considering the anticancer effect of the other molecules on lung cancer cells, it was seen as similar to the 5FU anticancer drug. However, their undesired toxic results on normal Beas2B cells are highly more than 5FU (GI50: 1.00 - 1.19, TGI: 1.03 - 1.92, and LC50: 1.77 - 9.41 µg/mL) (Table 3). Therefore, it was expressed that subjected molecules are not convenient for lung cancer therapy. If **2** (GI50: 1.04 - 1.89, TGI: 1.78 - 18.7, and LC50: >500 µg/mL), **3b** (GI50: 1.00 - 3.04, TGI: 8.13 - 324.8, and LC50: >500 µg/mL), **3c** (GI50: 1.05 - 2.98, TGI: 4.99 - 198.2, and LC50: >500 µg/mL), **3d** (GI50: 1.03 - 2.38, TGI: 1.36 - 26.6, and LC50: 23.50 - >500 µg/mL), and **3a** (GI50: 1.06 - 7.42, TGI: 9.52 - > 500, and LC50: >500 µg/mL) molecules examined their antiproliferative effect in terms of normal cells HC cells, it was seen that these molecules have safety (Tables 3). However, when examining Tables 2 and 3, it was seen that the anticancer activity exhibited by subjected molecules was found at a similar or higher level than the control anticancer drug 5FU in bone cancer cells while these caused a higher anticancer effect on cells (GI50: 1.04 - 2.38, TGI: 1.78 - 90.8, and LC50: > 500 µg/mL) (Table 2). When we look at the effects of these molecules, which stand out in terms of NCI60 survival parameters, it is seen that both GI50, TGI, and LC50 values are in the desired range only in the bone cancer cell lines. These findings indicate that these molecules are cancer-specific for these cancer types. Especially, when considering all treated

bone cancer cell lines, the **2** and **3b** molecules (GI50: 1.04 - 1.88, TGI: 1.78 - 10.6, and LC50: > 500 µg/mL for cancer cells and GI50 value 1.81- 3.02, TGI value 48.8 - >500, and LC50 value > 500 µg/mL for normal cells) is the most convenient one for further preclinical studies (Table 2 and 3).

Table 2. GI50, TGI, and LC50 values (as µg/mL) for tested compounds against MG63, Saos2, and SW1353*

Compound	MG63**			Saos2**			SW1353**		
	GI50	TGI	LC50	GI50	TGI	LC50	GI50	TGI	LC50
3e	1.04	1.32	7.47	1.03	1.23	3.82	1.00	1.09	2.91
2	1.05	2.03	>500	1.89	9.44	>500	1.04	1.78	>500
3g	1.16	1.95	18.2±0.9	1.09	1.48	5.62	1.01	1.13	2.74
3b	1.12	8.13	>500	1.39	10.6±0.5	>500	1.88	8.61	>500
3c	1.31	90.8±3.9	>500	1.20	4.99	>500	1.94	14.9±0.6	>500
3d	2.38	23.8±1.2	>500	1.05	1.59	62.2±2.8	1.03	1.36	23.5±1.1
3f	1.82	4.79	59.5±2.5	1.33	2.49	17.3±0.9	1.01	1.15	3.55
3a	7.42	>500	>500	1.21	>500	>500	1.43	9.52	>500
5FU	1.82	52.7±2.8	429.4±21	1.43	42.7±2.0	431.2±19	1.56	40.5±1.9	409.3±15

*Percent inhibition noted is mean values ± SDs of three independent measures.
** If percent inhibition is smaller than 10, the SD value is <0.5.

Table 3. GI50, TGI, and LC50 values (as µg/mL) for tested compounds on Beas2B and HC*

Compound	Beas2B**			HC**		
	GI50	TGI	LC50	GI50	TGI	LC50
3e	1.26	1.92	6.37	1.18	2.00	17.2±0.8
2	1.06	1.45	9.41	1.81	48.8±2.5	>500
3g	1.19	1.68	4.78	1.28	2.61	41.7±2.0
3b	1.00	1.05	2.34	3.02	>500	>500
3c	1.02	1.19	3.38	1.69	36.2±1.9	>500
3d	1.18	1.77	6.54	1.05	2.18	>500
3f	1.00	1.03	1.77	1.10	1.70	19.5±1.0
3a	1.09	1.46	4.74	1.04	>500	>500
5FU	1.50	52.7±2.0	428.9±17	1.66	57.2±2.3	433.6±18

*Percent inhibition noted is mean values ± SDs of three independent measures.
** If percent inhibition is smaller than 10, the SD value is <0.5.

3.2.2. Cytotoxic Activity of the New Molecules

The measurement of the cytoplasmic LDH enzyme passed into the extracellular environment as a result of newly synthesized molecule-induced membrane deformations provides some information about their cytotoxic activities.

Table 4. % Cytotoxicity for tested compounds at TGI concentrations against the cells*,**

Compound	A549	Calu1	H1650	MG63	Saos2	SW1353	Beas2B	HC
3e	38.45	28.02	25.02	36.18	39.51	38.57	36.22	36.37
2	18.83	29.10	22.17	35.14	29.59	37.46	40.36	15.42
3g	35.26	38.19	22.33	39.09	40.67	38.32	40.56	35.17
3b	13.54	7.55	2.92	24.23	20.49	23.04	39.67	4.06
3c	14.91	2.23	17.57	8.70	29.35	24.00	38.93	14.00
3d	18.17	38.45	29.68	18.52	37.14	39.13	37.86	18.73
3f	34.20	40.34	39.66	29.53	34.07	37.19	40.07	38.54
3a	19.51	20.37	10.84	5.33	4.11	28.39	38.00	5.61
5FU	14.83	16.74	15.30	14.76	15.81	13.46	15.08	15.12

The cytoplasmic lactate dehydrogenase activity is measured with the help of an LDH cytotoxicity kit. In this study, cytotoxicity induced by these molecules was measured using TGI concentrations. Accordingly, **2**, **3b**, **3c**, and **3d** molecules that were found to be effective in the MTT proliferation test showed moderate cytotoxicity values varying between about 4.06 – 18.73 % for HC

normal cell lines and 20.49 - 39.13 % bone cancer cells at TGI concentration (Table 4). However, the cytotoxic effects (varying between about 37.86 - 40.36 % for Beas2B normal cell lines and 2.23 – 38.45 % lung cancer cells at TGI concentration) of the tested **2**, **3b**, **3c**, and **3d** molecules on lung cancer cells were higher than 5FU (positive control) (Table 4).

Although these molecules are effective on lung cancer, these molecules are not suitable for further studies because they have very high cytotoxic effects on normal lung cells. However, if the high toxicity on normal cells is eliminated by chemical modifications to the molecules, then these molecules may be good anticancer candidates. The MTT and LDH assay results, which show the therapeutic and cytotoxic features, respectively, were evaluated together, it was vigorously expressed that **2**, **3b**, and **3c** show the most optimal antiproliferative and cytotoxic effect against bone cancer and normal cells compared to the positive control, 5FU (Tables 2, 3, and 4). Overall, these **2**, **3b**, and **3c** molecules are sufficiently toxic to bone cancer cell lines but safe against normal cells, creating an opportunity for further preclinical studies.

A structure-activity relationship was conducted in that imidazolium ionic liquid core containing different lengths of two N-bounding hydrocarbon chains led to different anti-cancer potentials. The results of the MTT test indicated that 3e (7 carbons long), 3f (8 carbons long), and 3g (9 carbons long) have high anticancer effects and apoptotic potentials. This means that if the hydrocarbon chain contains more than 7 carbons, the anticancer property of the compound increases. However, according to the LDH test results, 3a (3 carbons long), 3b (4 carbons long), 3c (5 carbons long), and 3d (6 carbons long) compounds were safe because of the low toxic effect. This means that if the hydrocarbon chain contains less than 6 carbons, the toxic property of the compound decreases. As a result, 3b (4 carbons long), the most optimum molecule with low toxicity and strong anticancer properties, may be a candidate molecule for further studies.

3.2.3. DNA Degradation

If a particular molecule initiates the apoptotic cascade, this causes enzymes called caspases to be activated. Activated caspases activate DNase, causing DNA cleavage, creating ~200 base pair fragments resembling a ladder shape on the agarose gel. This method helps detect DNA fragments to examine a cell's apoptotic status. Because, there was no DNA fragmentation in untreated cells (well 1), intact genomic DNA was visible near the well. When examining DNA laddering images, it is figured out that these compounds caused the formation of DNA fragments in treated A549 (A), MG63 (C), and Beas2B (B) cells compared to the untreated cells (Figure 1). However, it should be said that there is less fragmentation in the lung control cells (Beas2B (B)) compared to lung and bone cancer cells (A549 (A) and MG63 (C)). These findings said that tested compounds have more antiproliferative effects on lung and bone cancer cells than normal lung cells. Overall, these compounds may cause an apoptotic cascade in the cell.

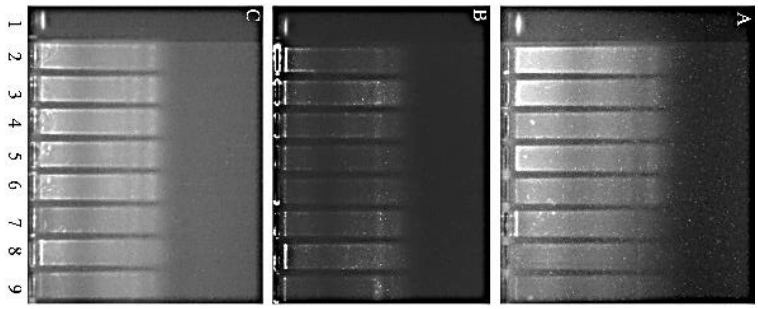

Figure 1. Effects of the 3a (**2**), 3f (**3**), 3d (**4**), 3c (**5**), 3b (**6**), 3g (**7**), 2 (**8**), and 3e (**9**) molecules on DNA laddering in A549 (A), Beas2B (B), and MG63 (C) cell lines. Well (**1**) is untreated control for all cells.

3.2.4 Effect of Substances on Cell Migration

The migration capacity of cells is an important characteristic of cancer development and is the target of new pharmacological agents. Cancer cells that have migration capacity can escape from the apoptosis mechanism. Therefore, one of the aims of newly developed pharmacological agents is to significantly reduce the migration capacity of cancer cells. According to the migration test performed in a time-dependent manner, it was understood that the molecules tested reduced the migration capacity of cancer cells to a certain extent compared to control cells (Figures 2 and 3). When the images of A549 cells obtained in the cell migration test were examined with ImageR, it was seen that **2**, **3b**, **3a**, and **3d** of the samples prevented significantly more migration than the control (Gap filling rate 13.40% - 36.06%) (Figure 2, Table 5). When the results are evaluated as a % difference for MG63 cells, it is understood that other molecules are the closest value to the control (Figure 3, Table 5). Therefore, it may speculate that when these molecules exert their effect on MG63 cells, they do not prefer the target of migration. They may be using other anticancer mechanisms of action, such as apoptosis, instead.

Table 5. Migration analysis of the molecules with the ImageR (% Area)

Compound	A549 cell line				MG63 cell line			
	Gap of Day 0	**Gap of Day 1**	**Gap of Day 2**	**Gap filling rate**	**Gap of Day 0**	**Gap of Day 1**	**Gap of Day 2**	**Gap filling rate**
2	70.45	58.14	35.14	35.31	82.18	50.11	4.87	77.30
3b	46.90	52.76	10.83	36.06	72.37	54.57	0	72.37
3a	58.38	45.85	44.97	13.40	74.83	45.92	0	74.83
3d	62.25	52.88	39.25	22.99	82.46	34.71	0	82.46
Control 1	57.94	31.51	0	57.94	76.56	51.64	0	76.56
Control 2	56.72	32.47	0	56.72	72.10	49.35	0	72.10

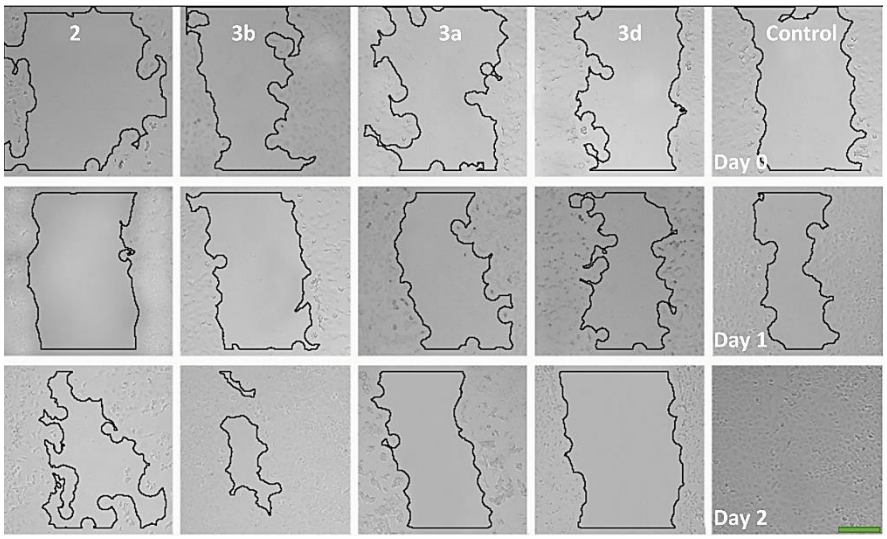

Figure 2. Effects of **2**, **3b**, **3a**, and **3d** on cell migration on A549 cell lines. The scale is 100 µm

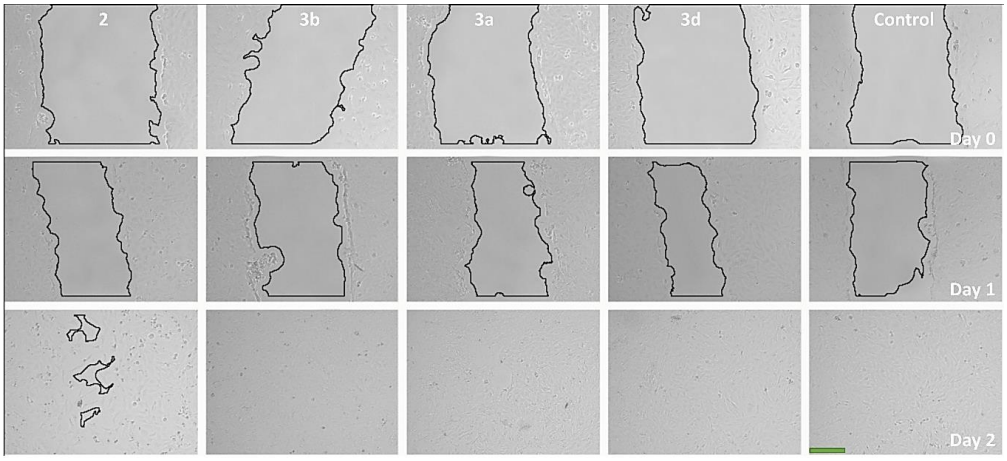

Figure 3. Effects of **2**, **3b**, **3a**, and **3d** on cell migration on MG63 cell lines. The scale is 100 µm

3.2.5 Effect of the New Molecules on Cell Morphology

In this study, the morphological effects of **2** and **3f** at two different concentrations on lung cancer cells (A549, Calu1, and H1650), bone cancer cells (Saos2, MG63, and SW1353), normal lung cells (Beas2B), and normal chondrocyte cells (HC) were observed and imaged 24 hours after application. Observed morphological alteration images here were clearly distinguished in all cell lines treated with the **2** and **3f** at two different concentrations (32 and 64 µg/mL). Some of them like weak cell attachment or reduction in cell volume, floating cells, cell rounding, cell aggregation, granular formation, cellular shrinkage, and disintegration of cell clumps were observed in the vast majority of the cells (Figures 4 and 5). The changes that occurred in the cell morphology by applying two different concentrations of **2** and **3f** molecules indicate that the effect mechanism of these molecules including apoptosis is in line with the MTT, LDH, DNA degradation, and cell migration test results of it.

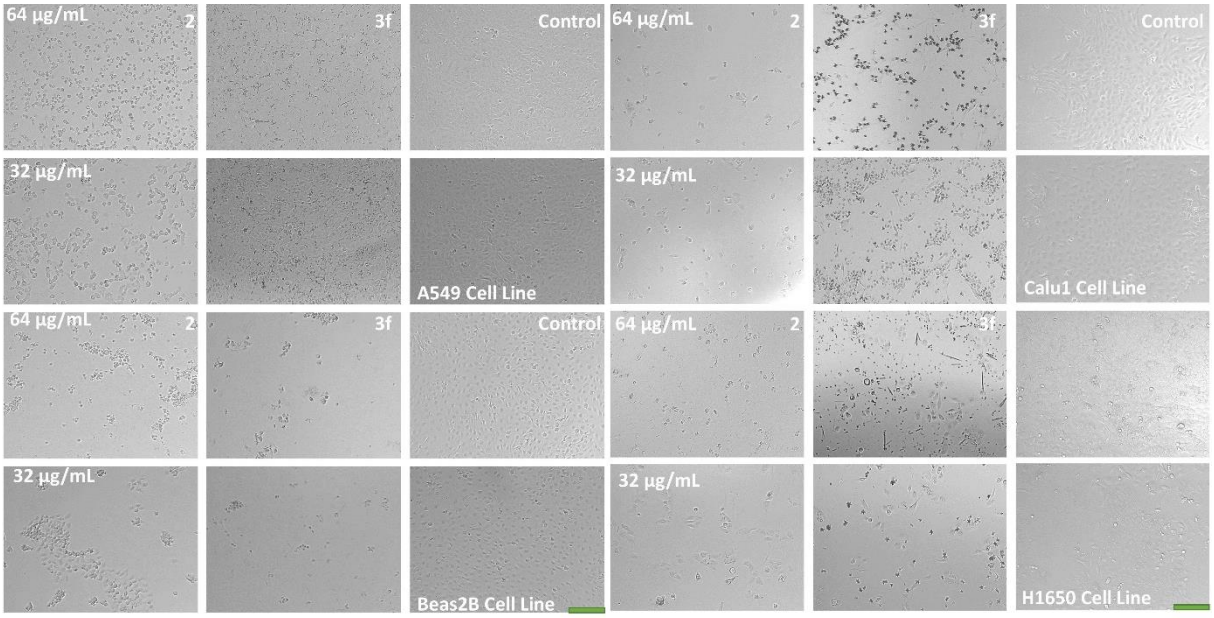

Figure 4. Effect of **2** and **3f** at two different concentrations on the morphology of A549, Beas2B, Calu1 and H1650 cell lines. DMSO treated cells as controls. The scale is 100 µm.

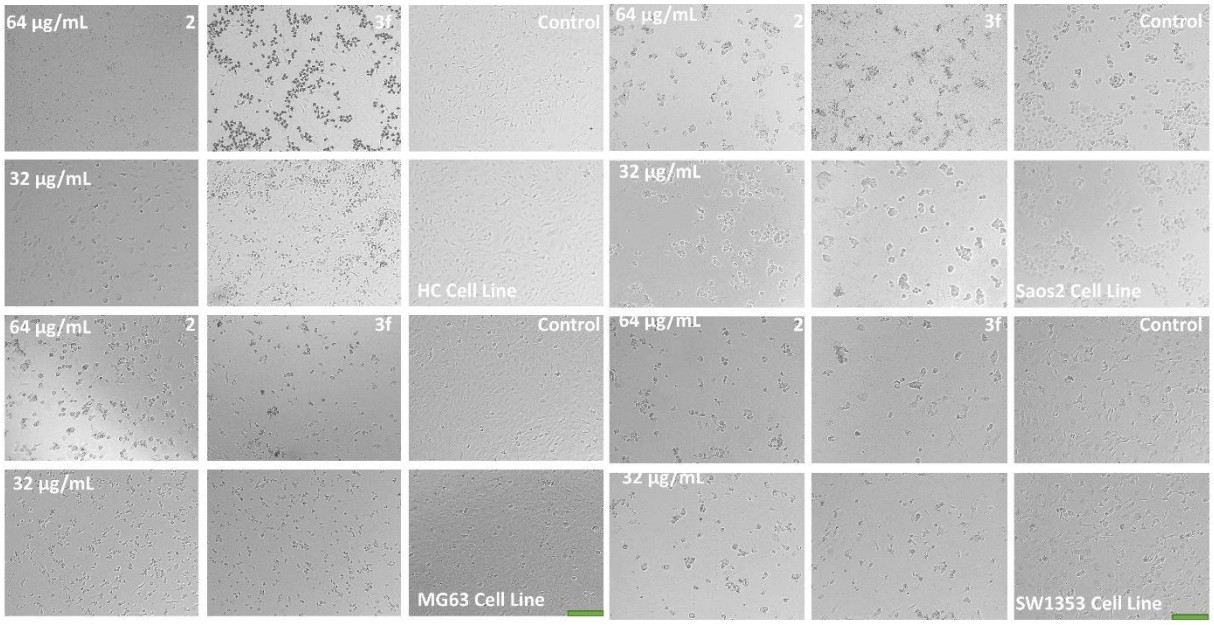

Figure 5. Effect of **2** and **3f** at two different concentrations on the morphology of HC, MG63, Saos2, and SW1353 cell lines. DMSO treated cells as controls. The scale is 100 µm.

3.3. Antimicrobial Activity

The in vitro antimicrobial activity of the synthesized compounds was evaluated against a range of microorganisms, including four Gram-positive bacteria (*B. cereus*, *B. subtilis*, *S. aureus*, *E. faecalis*), four Gram-negative bacteria *(E. coli*, *Y. pseudotuberculosis*, *P. aeruginosa*, *K. pneumoniae*) and two yeast-like fungi (*C. albicans*, *C. tropicalis*). Table 6 showed the minimum inhibitory concentrations (MIC) of the newly synthesized compounds together with those of standard antibiotics against the eight bacteria and two yeast strains.

As a result of the MIC experiments, DMSO was found not to inhibit the growth of the tested microorganisms. After a comprehensive evaluation of the results of the antimicrobial activity of the compounds, it was found that compounds **2** and **3a** had low activity, **3b** and **3c** had moderate activity, **3d** and **3e** had high activity and **3f** and **3g** had very high activity.

The MIC values obtained for compounds **2** and **3a** against all microorganisms tested are between 625 and 1250 µg/mL, indicating low activity. While compounds **3b** and **3c** have high MIC values (156.2 µg/mL) against fungi, indicating low antifungal activity, their MIC values against bacteria range from 78.1 to 312.5 µg/mL, indicating moderate antibacterial activity. In particular, the MIC values of compound **3b** against *B. cereus*, *B. subtilis*, *P. aeruginosa* and *K. pneumoniae* are lower than those of compound **3c**, and compounds **3b** and **3c** have the same MIC value (78.1 µg/mL) against *Y. pseudotuberculosis*, *E. coli*, *S. aureus* and *E. faecalis*. Compounds **3d** and *3e*, which have high activity, show lower MIC values and higher antimicrobial activity against *Y. pseudotuberculosis*, *P. aeruginosa*, *S. aureus* and *E. faecalis* compared to the standard antibiotic (ampicillin).

Among all synthesized compounds, compound **3g** has the lowest MIC values and the highest activity against all tested microorganisms. The MIC values for compound **3g** against tested microorganisms range between 2.4 and 9.8 µg/mL. These MIC values are significantly lower than those of the standard antibiotics ampicillin (8-128 µg/mL) and fluconazole (8 µg/mL), indicating that compound **3g** is much more effective than standard antibiotics against all tested microorganisms. Additionally, Compound **3f**, which exhibits very high activity, has been determined to possess lower MIC values than standard antibiotics against all microorganisms except *E. coli*, indicating higher antimicrobial activity.

In summary, while each compound displays varying degrees of antimicrobial activity, Compound 3e and Compound 3f stand out for their notable efficacy against a wide range of microorganisms, making them particularly promising for further investigation and development.

Table 6. Antibacterial activity of compounds 2, 3a-g and antibiotics against tested microorganisms.

	Compounds								Antibiotics	
Microorganisms	**2**	**3a**	**3b**	**3c**	**3d**	**3e**	**3f**	**3g**	**Amp.**	**Fluc.**
B. cereus	625	1250	39.1	78.1	19.3	9.8	9.8	4.9	15	N.T
B. subtilis	1250	1250	156.2	312.5	39.1	39.1	9.8	4.9	10	N.T
Y. pseudotuberculosis	1250	1250	78.1	78.1	9.8	9.8	2.4	2.4	18	N.T
K. pneumoniae	1250	1250	156.2	312.5	19.5	19.5	9.8	9.8	16	N.T
E. coli	1250	1250	78.1	78.1	9.8	19.5	9.8	4.9	8	N.T
P. aeruginosa	1250	1250	39.1	78.1	9.8	4.9	9.8	2.4	128	N.T
S. aureus	1250	625	78.1	78.1	9.8	9.8	9.8	4.9	10	N.T
E. faecalis	1250	1250	78.1	78.1	9.8	9.8	2.4	2.4	10	N.T
C. albicans	625	625	156.2	156.2	9.8	9.8	4.9	4.9	N.T	8
C. tropicalis	1250	1250	156.2	156.2	19.5	19.5	4.9	4.9	NT	8

Minimal inhibition concentration (MIC) values were given as μg/mL. N.T: not tested.

3.4. Molecular Docking

Molecular docking is a crucial element of early-stage drug development. It allows for the efficient evaluation of a multitude of potential drug candidates, the prediction of their interactions with target proteins, and the determination of the strength of these interactions. This approach not only saves valuable time and resources compared to experimental screening but also aids in the prioritization of promising compounds for further exploration.[13] In this investigation, we conducted molecular docking to elucidate the interactions between compound 3a and both the Epidermal Growth Factor Receptor (EGFR) and the Vascular Endothelial Growth Factor Receptor 1 (VEGFR1). EGFR, also known as Proto-oncogene c-ErbB-1, is a vital transmembrane protein that acts as a receptor for Epidermal Growth Factor family members. This integral cell membrane protein spans both normal and malignant epithelial cell membranes and contains a tyrosine-specific protein kinase domain. Its extracellular region binds EGF, while its intracellular carboxy-terminal region hosts tyrosine kinase activity.[14] Mutations affecting EGFR expression or activity can contribute to cancer development in various cancer types.[15] Conversely, VEGFR-1, a member of the VEGFR family, binds VEGF-A, PlGF, and VEGF-B. What sets it apart is its unique expression of two types of mRNA, one encoding a full-length receptor and the other producing a shorter, soluble protein known as soluble VEGFR-1. Additionally, VEGFR-1 is a crucial protein receptor involved in controlling blood vessel growth, making it a significant focus of medical research, particularly in angiogenesis-related treatments and cancer research, where it plays a pivotal role in regulating tumor blood vessel growth.[16] The successful docking simulations demonstrated that 3a exhibited strong binding affinities to both receptors. The lower the binding energy, the stronger the ligand's interaction with the protein. In this study, Erlotinib served as the reference drug for EGFR, while Dovitinib and Axitinib were employed for VEGFR-1, and their docking results were compared with those of 3a Erlotinib, an EGFR tyrosine kinase inhibitor, is employed in treating various cancer types, including non-small cell lung cancer and pancreatic cancer.[17] In contrast, Dovitinib targets type III-V RTKs, such as VEGFR and PDGFR, which play critical roles in promoting tumor cell proliferation and survival in specific cancer cells .[18]Axitinib, a second-generation tyrosine kinase inhibitor, selectively impedes vascular endothelial growth factor receptors (VEGFR-1, VEGFR-2, VEGFR-3), effectively suppressing angiogenesis, tumor growth, and metastasis.[19] The docked poses for 3a and the reference molecules were evaluated, and the pose with the lowest binding free energy and inhibition constant was chosen (Table 7). The completion of the docking procedure between the ionic compound and EGFR resulted in a computed binding free energy of -8.28 kcal/mol, with an inhibition constant of 857.88 nM, showing a remarkable resemblance to the reference compound Erlotinib. Upon closer examination of the interactions between the ionic compound and the EGFR binding site, it became apparent that a conventional hydrogen bond formed at a distance of 2.30 Å with the Asp831 residue.

Additionally, four carbon hydrogen bonds, two Pi-anion bonds, two alkyl bonds four and Pi-alkyl bonds were formed, six of which exhibited atomic distances less than 4 Å. Further investigation into the key amino acids to which both **3a** and Erlotinib bind revealed a substantial overlap in the amino acids involved. These shared amino acid residues include Val702, Lys721, Gln767 and Leu764. Conversely, when examining the binding mode of 3a with the VGFR-1 receptor, it was found to exhibit a binding energy of -9.84 kcal/mol and a K_i value of 61.26 nM. A comparison with reference drugs indicated a more favorable score than dovitinib and a score nearly equivalent to axitinib.

Analysis of the interacting key residues showed that both the compound **3a** and reference drugs engaged with similar residues. The interactions between the **3a** and VGFR-1 resulted in the formation of one conventional hydrogen bond with a distance of 1.70 Å within the Glu878 residue. Furthermore, it was observed that one carbon hydrogen bond, four pi-alkyl bonds and four alkyl bonds were established. The docked poses of the ligand binding to both receptors, the interacting residues, and the interactions are visually presented in Figures 6 and 7. This in silico analysis revealed the potential of the compound 3a to inhibit target proteins. Consequently, the current compound exhibits substantial promise for the design and development of novel and more effective drugs.

Table 7. Predicted binding poses of compound 3a against receptor proteins.

Protein	**Ligand**	**Free Binding Energy (kcal/mol)**	**K_i value**	**Number of HBs**	**Number of Closest Residues**	**Interacting Key Residues**
Epidermal growth factor receptor **(EGFR)** 1M17, (Res:2.60 Å, Chain:A)	3a	-8.28	857.88 nM	4	10	Phe699, Val702, Lys721, Leu764, Gln767, Arg817, Asn818, Asp831,
	Erlonitib*	-7.68	2.35 μM	3	9	Leu694, Val702, Ala719, Lys721, Met742, Leu764, Thr766, Gln767, Met769, Cyc773, Leu820
Vascular endothelial growth factor receptor 1, 3HNG (Chain:A, Res:2.70 Å)	3a	-9.84	61.26 nM	2	16	Leu833, Ala859, Glu878, Ile881, Leu882, Val892, Cys912, Leu1029, Cys1039
	Dovitinib*	-8.71	410.99 nM	2	8	Leu833, Ala859, Lys861, Glu878, Leu882, Val892, Val909, Tyr911, Cys912, Leu1029, Cys1039,
	Axitinib*	-10.67	15.03 nM	3	8	Val841, Lys861, Glu878, Ile881, Leu882, Val891, Val892, Val907, Cys1018, Ile1038, Cys1039, Asp1040, Phe1041

*Reference molecules

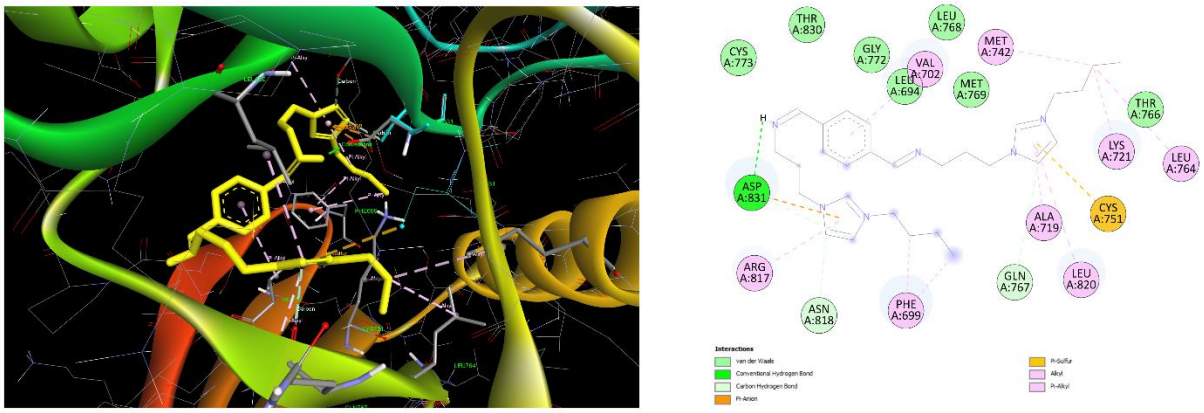

Figure 6. Binding orientations of compound3a in both 2D and 3D conformations with the critical amino acid residues situated within the binding site of EGFR (1M17).

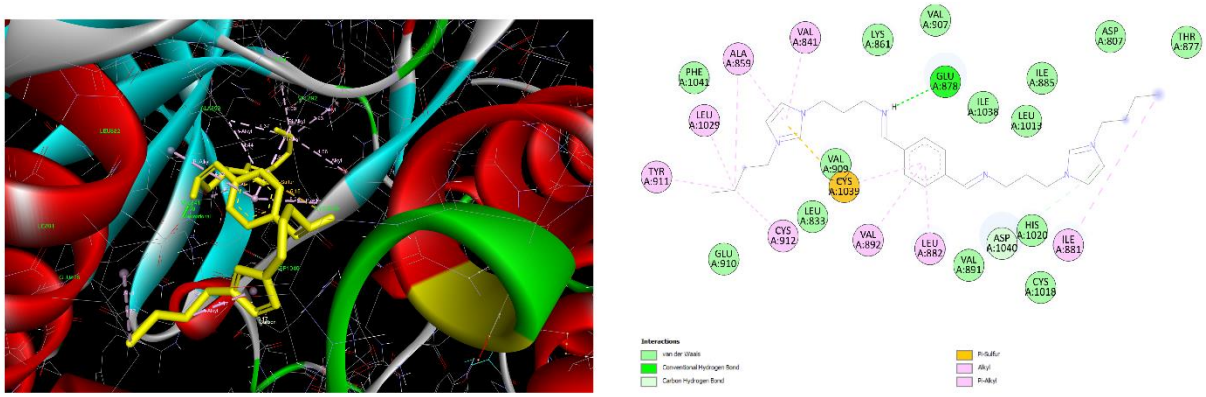

Figure 7. Binding orientations of compound 3a in both 2D and 3D conformations with the critical amino acid residues situated within the binding site of VEGFR-1 (3HNG).

4. Conclusion

In this study, In this study, bis Schiff base with imidazole (**2**) and bis imidazolium ionic liquids (**3a**-**g**) were synthesized. The new compounds were characterized by IR, ^{1}H and ^{13}C NMR spectroscopic methods. The anticancer effects of the synthesized molecules were tested. Compared to other molecules and 5FU (positive control), compounds **3e**, **3g** and **3f** showed strong anticancer activity against all cancer cell lines (GI50: 1.0 - 1.82, TGI: 1.09 - 4.79 and LC50: 2.74 – 59.5 µg/mL), but they also caused a highly cytotoxic effect on normal lung cells Beas2B and normal cartilage cells HC (GI50: 1.0 - 1.28, TGI: 1.03 - 2.61 and LC50: 1.77 - 41.7 µg/mL). While each compound exhibited varying degrees of antimicrobial activity, compounds **3e** and **3f** were characterized by their remarkable efficacy against a wide range of microorganisms, making them particularly promising for further investigation and development. In the molecular docking study, analysis of the interacting key residues showed that both compound 3a and the reference drugs interacted with similar residues. The interactions between 3a and VGFR-1 resulted in the formation of a conventional hydrogen bond with a distance of 1.70 Å within the Glu878 residue.

Acknowledgements

This study was supported by grants from Karadeniz Technical University (KTU FBA-2023-10705).

Supporting Information

Supporting information accompanies this paper on http://www.acgpubs.org/journal/organic-communications

ORCID
Fatih Çelik: 0000-0001-5510-3494
Yasemin Ünver: 0000-0001-5834-3223
Ali Aydın: 0000-0002-9550-9111
Halil İbrahim Güler : 0000-0002-7261-6790
Kadriye İnan Bektaş*:* 0000-0002-5909-588X

References

[1] Tanak, H.; Köysal, Y.; Ünver, Y.; Yavuz, M.; Işık, Ş.; Sancak, K. Experimental and DFT studies of ethyl N'-3-(1H-imidazol-1-yl) propylcarbamoyl benzohydrazonate monohydrat. *Struct. Chem*. **2009**, *20*, 409-416.

[2] Tanak, H.; Köysal, Y.; Ünver, Y.; Yavuz, M.; Işık, Ş.; Sancak, K.An Experimental and DFT computational study on 4-(3-(1H-imidazol-1-yl)propyl)-5-methyl-2H-1,2,4-triazol-3(4H)-one monohydrate. *Mol. Phys.* **2010**, *108*, 127-139.

[3] Ünver, Y.,; Sancak, K.; Tanak, H.; Değirmencioğlu, İ.; Düğdü, E.; Er, M.; Işık, Ş. 5-Benzyl-4-[3-(1H-imidazol-1-yl)propyl]-2H-1,2,4-triazol-3(4H)-ones: Synthesis, spectroscopic characterization, crystal structure and a comparison of theoretical and experimental IR by DFT calculation. *J. Mol. Struct.* **2009**, *936*, 46-55.

[4] Sancak, K.; Ünver, Ü.; Tanak, H.; Değirmencioğlu, İ.; Düğdü, E.; Er, M.; Işık, Ş. The Synthesis of some new imidazole and triazole derivatives: Crsytal structure and DFT-TDDFT investigation on electronic structure. *J. Incl. Phenom. Macrocycl. Chem.* **2010**, *67*, 325-334.

[5] Ustabas, R.; Süleymanoğlu, N.; Tanak, H.; Alpaslan, Y. B.; Ünver,Y.; Sancak, K. Experimental and theoretical studies of the molecular structure of 4-(3-(1H-imidazol-1-yl)propyl)-5-p-tolyl-2H-1,2,4-triazol-3(4H)-one. *J. Mol. Struct.* **2010**, *984*, 137-145.

[6] Ünver, Y.; Süleymanoğlu, N.; Ustabaş, R.; Bektaş, K. İ.; Bektaş, E.; Güler, H. İ. 3-(5-(1*H*-imidazol-1-yl) pent-1-en-1-yl)-9-ethyl-9*H*-carbazole: Synthesis, characterization (IR, NMR), DFT, antimicrobial-antioxidant activities and docking study. *J. Biomol. Struct. Dyn.* **2022**, *40*, 1990–13000.

[7] Abdel-Wahab, B. F.; Awad, G. E. A.; Badria, F. A. Synthesis, antimicrobial, antioxidant, anti-hemolytic and cytotoxic evaluation of new imidazole-based heterocycles. *Eur. J. Medi. Chem.* **2011**, *46*, 1505-1511.

[8] Rani, N.; Sharma, A.; Singh, R. Imidazoles as promising scaffolds for antibacterial activity: A review. *MiniRev. Med. Chem.* **2013**, *13*(*12*), 1812-1835.

[9] Wright, S.W.; Harris, R.R.; Collins, R.J.; Corbett, R.L.; Green, A.M.; Wadman, E.A.; Batt, D.G. Novel l-(pyridylphenyl)-lphenyl- 2-imidazolyl ethanols with topical antiinflammatory activity. *J. Med. Chem.* **1992**, *35*, 3148-3155.

[10] Jain, R.; Vangapandu, S.; Jain, M.; Kaur, N.; Singh, S.; Singh, P.P. Antimalarial activities of ring-substituted bioimidazoles. *Bioorg. Med. Chem. Lett*. **2002**, *12*, 1701-1704.

[11] Soujanya, Y.; Sastry, G.N. Theoretical elucidation of the antioxidant mechanism of 1,3-dihydro-1-methyl-2*H*-imidazole-2-selenol (MSeI). *Tetrahedron Lett.* **2007**, *48*, 2109-2112.

[12] Hussain, T.; Siddiqui, H.L.; Rehman, M.Z.; Yasinzai, M.M.; Parvez, M. Anti-oxidant, anti-fungal and anti-leishmanial activites of novel 3-[4-(1*H*-imidazol-1-yl)phenyl]prop-2-en-1-ones. *Eur. J. Med Chem.* **2009**, *44*, 4654-4660.

[13] Goreci, C.Y. Synthesis and comparative spectroscopic stud-ies, HOMO–LUMO analysis and molecular docking studies of 3,3-(1,4-phenylene)bis[2-(6-chloropyridin-3-yl)prop–2-enenitrile] based on DFT. *J. Mol. Struct.* **2022**, *1263*, 133149 .

[14] Herbst, R.S. Review of epidermal growth factor receptor biology. *Int. J. Radiation Oncol. Biol. Phys.* **2004**, *59*, 21–26.

[15] Moore, Zhang, H.; Berezov, A.; Wang, Q.; Zhang, G.; Drebin, J.; Murali, R.; Greene, M.I. ErbB receptors: from oncogenes to targeted cancer treatment. *J. Clin. Investig*. **2007**, *117 (8)*, 2051–2058.

[16] Shibuya, M. Vascular endothelial growth factor receptor-1 (VEGFR-1/Flt-1): a dual regulator for angiogenesis. *Angiogenesis* **2006**, *9*, 225–230.
[17] Rocha-Lima, C.M.; Raez, L.E. Erlotinib (tarceva) for the treatment of non-small-cell lung cancer and pancreatic cancer. *P T.* **2009**, 3*4(10*), 554-564.
[18] Lee, C.K.; Lee M.E.; Le, W.S.; Kim, J.M.; Park, K.H.; Kim, T.S.; Lee, K.Y.; Ahn, J.B.; Chung, H.C.; Rha, S.Y. Dovitinib (TKI258), a multi-target angiokinase inhibitor, is effective regardless of KRAS or BRAF mutation status in colorectal cancer. *Am. J. Cancer Res*. **2014**, *5(1),* 72-86.
[19] Kelly, R.J.; Rixe, O. Axitinib-a selective inhibitor of the vascular endothelial growth factor (VEGF) receptor. *Target Oncol*. **2009**, *4(4),* 297-305.